



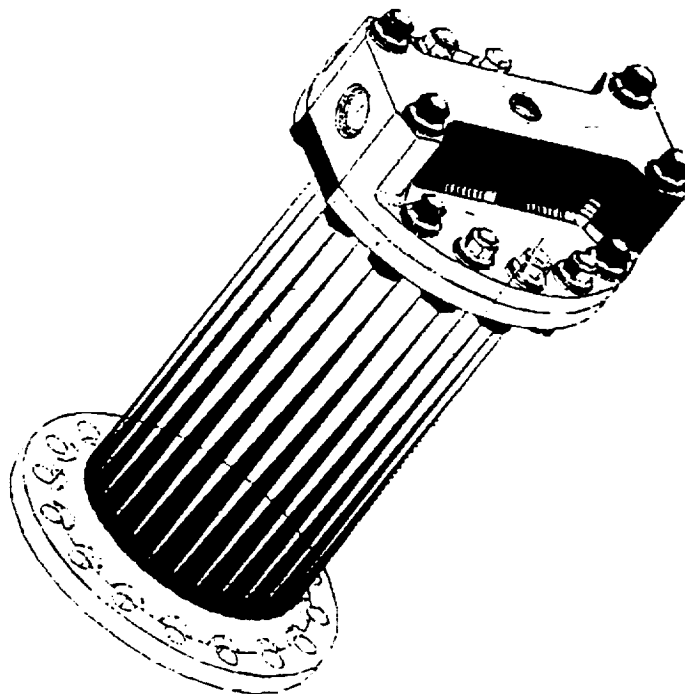
CONF. PAPER
IN-20
© WAIVED
375 884

AIAA 98-3366

**Thermal Analysis and Testing of
Fastrac Gas Generator Design**

H. Nguyen

*NASA Marshall Space Flight Center,
Huntsville, AL 35812*



**34th AIAA/ASME/SAE/ASEE
Joint Propulsion Conference & Exhibit
July 13-15, 1998/Cleveland, OH**

Thermal Analysis and Testing of Fastrac Gas Generator Design

H. Nguyen*

NASA Marshall Space Flight Center, Huntsville, AL 35812

Abstract

The Fastrac Engine is being developed by the Marshall Space Flight Center (MSFC) to help meet the goal of substantially reducing the cost of access to space. This engine relies on a simple gas-generator cycle, which burns a small amount of RP-1 and oxygen to provide gas to drive the turbine and then exhausts the spent fuel.

The Fastrac program envisions a combination of analysis, design and hot-fire evaluation testing. This paper provides the supporting thermal analysis of the gas generator design. In order to ensure that the design objectives were met, the evaluation tests have started on a component level and a total of 15 tests of different durations were completed to date at MSFC. The correlated thermal model results will also be compared against hot-fire thermocouple data gathered.

Introduction

DURING the past several years, increasing emphasis has been given to the development of a low-cost space transportation system.¹ Two key areas with potential for limiting the cost of future space transportation systems are efficient engine development and optimal utilization of inexpensive propellants, such as the LOX(liquid oxygen) /RP-1. To make further progress in the above key areas, in 1996 MSFC sponsored the Low-Cost Boost Technology Project,² the centerpiece of which is the development of a economical reusable engine derived from previous technology programs for turbopump³⁻⁴ and chamber⁵ to serve as the main propulsion system (MPS) for the X-34 vehicle.

The X-34 MPS features, among many others, a conventional gas-generator cycle and simple robust design using commercial off-the-shelf components to encourage nontraditional vendors and small corporations to introduce commercial design and manufacturing processes advantageous for space transportation. Another goal set for the MPS is its minimal maintenance to meet operability requirements. Interested readers may consult other documents⁶⁻⁷ for more details about the design and development of the MPS. The rest of

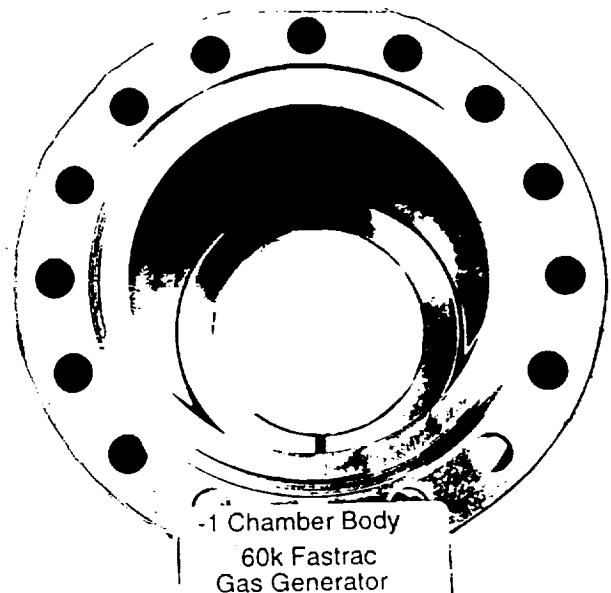


Fig. 1 Combustion Chamber

this paper focuses on the Fastrac gas generator design, thermal analysis and testing results.

Gas Generator Design

The Fastrac gas generator baseline configuration consists of a faceplate brazed to an injector assembly and a combustion chamber.

The uncooled combustion chamber is a cylinder whose length and diameter are 8.875 in. and 3.535 in., respectively. Turbulent mixing near the chamber wall is further promoted by the slotted turbulence ring (Figure 1), whose exact distance from the faceplate is going to be determined by hot-fire testing. This chamber is made of Hastelloy-X, a nickel-base alloy. The higher thermal conductivity (compared to steel's) of nickel provides additional design margin since local hot spots are better diffused. Other materials selection criteria for this project are

- Low-cost and easily obtainable;
- Easily weldable;

*Senior Member AIAA

Copyright © 1998 by the American Institute of Aeronautics and Astronautics, Inc. No copyright is asserted in the United States under Title 17, U.S. Code. The U.S. Government has a royalty-free license to exercise all rights under the copyright claimed herein for Governmental Purposes. All other rights are reserved by the copyright owner.



Fig. 2 Injector/Faceplate

- Brazeable by demonstrated processes;
- Compatible with LOX, RP-1, and the resulting combustion products.

The brazed injector assembly (Fig. 2) is a single-piece, 304L-stainless steel manifold body brazed to a 3.535-inch diameter faceplate constructed of oxygen-free, high-conductivity copper. The selected materials met the listed criteria. Each injector element is composed of one pair of self-impinging RP-1 orifices shielding a single oxidizer orifice in a conventional fuel-oxidizer-fuel (F-O-F) triplet arrangement. Table 1 gives the orifice diameters and other pertinent design parameters.

For testing purpose, a turbine simulator (Fig. 3) was included to supply the back pressure. A chamber spacer (Fig. 4) was also utilized to allow tests on a longer chamber. An instrumentation rake at the exit plane contains six thermocouple probes for turbine inlet temperature distribution measurements in the radial direction, and two pressure probes (Fig. 5). The disassembled and assembled test hardware are shown by Fig. 6 and Fig. 7.

In the following sections, the objectives of thermal analysis, the governing equation, and solution procedure will be taken up.

Objectives

The thermal analysis has several primary aims:

- Minimize the RP-1 freezing in the injector manifold (avoid unpredictable combustion characteristics)
- Provide adequate cooling of the injector faceplate
- Maintain hardware structural integrity i.e. no melting

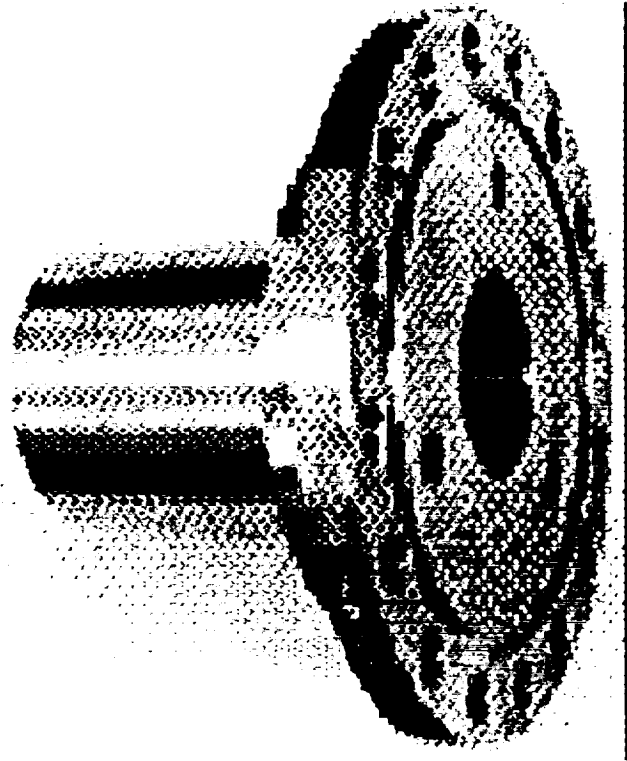


Fig. 3 Turbine Simulator

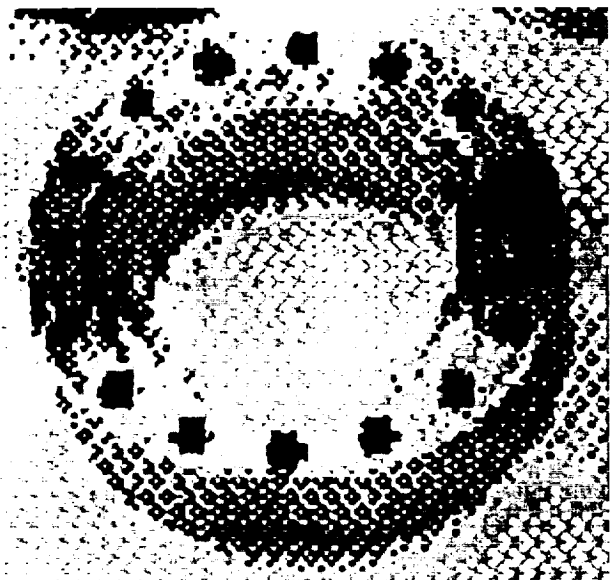


Fig. 4 Chamber Spacer

Nominal Chamber Pressure, <i>psia</i>	575
Oxidizer Flowrate, <i>lbm/sec</i>	1.64
Fuel Flowrate, <i>lbm/sec</i>	5.46
Mixture Ratio	0.3
Gas Exit Temperature, $^{\circ}R$	1600
Exit Temperature Profile, $^{\circ}R$	± 50
Number of Oxidizer Orifices/Dia., <i>in.</i>	42/0.034
Number of RP-1 Orifices/Dia., <i>in.</i>	84/0.047
LOX Mean Injection Velocity, <i>ft/s</i>	90
LOX Injection Pressure, <i>psia</i>	702
RP-1 Mean Injection Velocity, <i>ft/s</i>	107
RP-1 Injection Pressure, <i>psia</i>	702

Table 1 Design Parameters

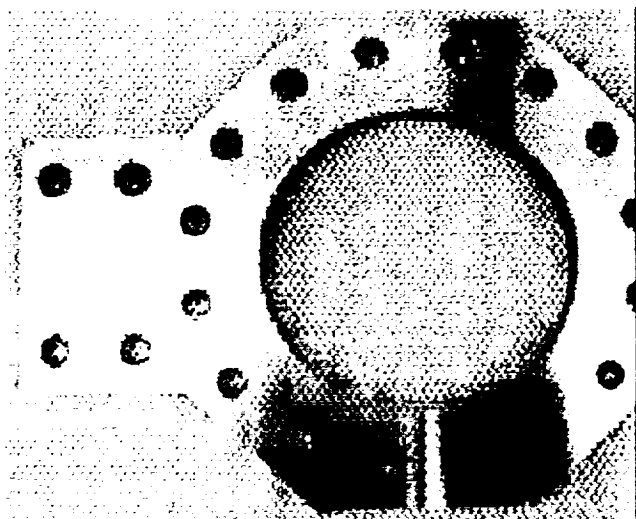


Fig. 5 Instrumentation Ring

- Supply temperature distribution for the subsequent stress analysis

The stress analysis is the subject of a separate study and will not be reported here.

Governing Equation

The governing differential equation⁸ for the conduction of heat in solid is

$$\rho c_p \frac{\partial T}{\partial t} = \nabla \cdot (k \nabla T) + q_v$$

where

c_p = specific heat

k = thermal conductivity

T = temperature

t = time

ρ = density

q_v = volumetric rate of internal heat generation

The specific heat c_p is a function of T , and is related to internal energy, U , through

$$c_p = \frac{dU}{dT}$$

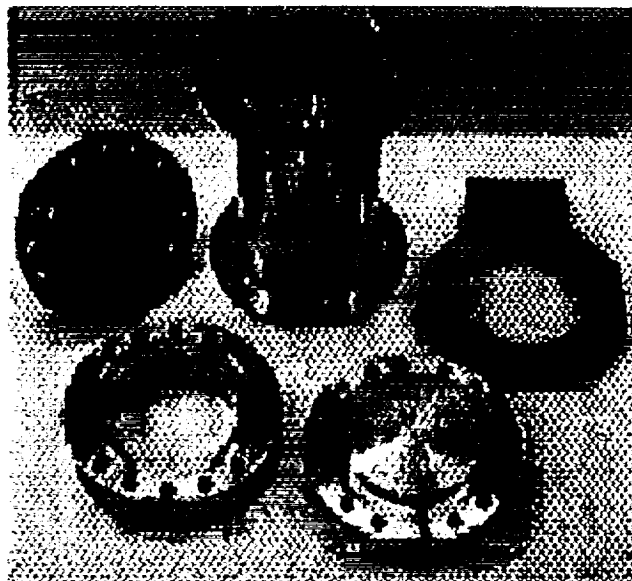


Fig. 6 Gas Generator Components

For most practical designs using many types of materials and operating over a wide range of T , temperature-dependent and spatial variations of thermal conductivity k must be considered. The resulting problem is nonlinear with boundary conditions specified on complex boundary.

Solution Procedure

The PATRAN⁹ commercial software was utilized to automate the tasks of modeling complicated geometry, imposing boundary conditions and material properties, and post-processing a massive amount of analysis results for a multi-dimensional configuration.

Figure 8 shows the solution procedure used in the thermal analysis. For basic mesh generation, the only required information is the desired element size and the boundary geometry for each material. PATRAN produces the nodal points, the conductors linking those nodes, and outputs the required lines for a SINDA thermal model.

SINDA¹⁰ solves the nonlinear heat conduction equation shown earlier using a lumped parameter finite-difference method where the geometry to be modeled is divided into lumps of mass called *nodes* that are connected to each other with PATRAN-generated conductors. The output file containing the temperature distribution from the SINDA calculation can be post-processed by PATRAN after each successful run.

Figure 9 shows a two-dimensional axisymmetric grid of the gas generator generated by PATRAN.

Hot-fire Testing

The primary goal of this component-level test is to evaluate and improve, if necessary, the baseline gas generator design (Fig. 7) for the Fastrac engine. More specifically, the tests are to describe

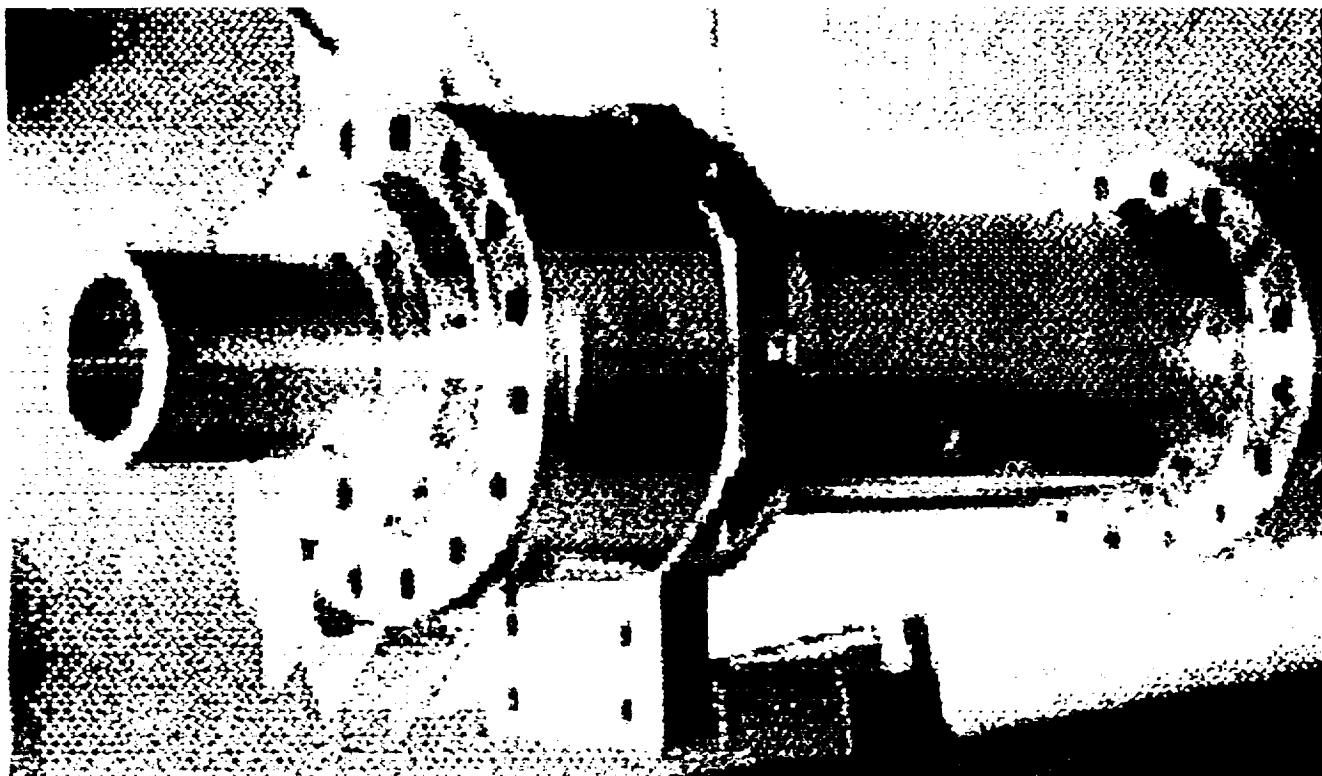


Fig. 7 Test Article

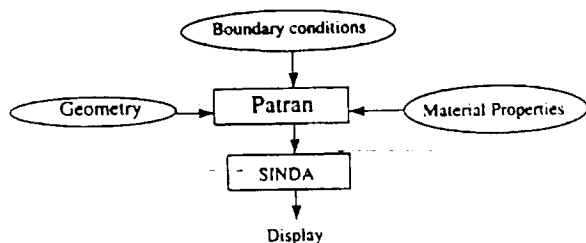


Fig. 8 Thermal Analysis Procedure

- Hot-gas temperature distribution at the inlet of the turbine simulator
- Performance based on measured flow rates of propellants, chamber pressure

The target for each of the above is outlined in Table 1.

The propellant flow was regulated using cavitating venturis. These devices provide a constant mass flow for a given inlet pressure and density. Propellants are provided in a pressure-fed mode.

Instrumentation on the test stand monitored all critical operating parameters. Test stand instrumentation included propellant tank pressures, feedline pressures and temperatures, and propellant flow rates. Engine instrumentation included chamber pressure, ac-

celerometers, propellant inlet pressures, fuel injector manifold temperature, and external skin temperature. No thrust measurement was attempted. Test data were made available to analysts as soon as the test ended.

Testing¹¹ was performed at MSFC Test Stand 116. A total of 15 tests were completed to date. Tables 2-5 show the duration, chamber pressure, and mixture ratio measured for each test.

Test Number	01	02	03	04
Test Duration, sec.	7.5	7.5	5.8	13.8
Mainst. Dur., sec.	0.	0.	2.0	10.0
Chamber Press., psig	85	135	475	470
Mainst. Mix. Ratio	-	-	0.29	0.29

Table 2 Tests 1-4 Summary

Test Number	05	06	07	08
Test Dur., sec.	3.8	63.8	153.8	103.8
Mainst. Dur., sec.	1.0	6.0	150.0	100.0
Cham. Pr., psig	477	534	530	535
Mainst. M.R.	0.30	0.30	0.30	0.31

Table 3 Tests 5-8 Summary

The maximum hot-gas temperature gradient measured at the turbine simulator inlet was 64 deg. F. The minimum was 28 deg. F. The ± 50 deg. F target (Table 1) was reached for most tests.

Test Number	09	10	11	12
Test Dur., sec.	153.9	7.6	63.8	23.8
Mainst. Dur., sec.	150.0	2.0	60.0	20.0
Cham. Pr., psig	520	475	483	480
Mainst. M.R.	0.30	0.24	0.25	0.25

Table 4 Tests 9-12 Summary

Test Number	13	14	15
Test Duration, sec.	63.9	63.8	33.9
Mainstage Dur., sec.	60.0	60.0	30.0
Chamber Press., psig	470	454	475
Mainstage Mix. Ratio	0.25	0.33	0.25

Table 5 Tests 13-15 Summary

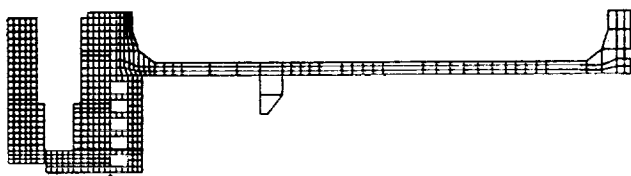


Fig. 9 2-D Patran Grid

Calculation Results and Discussion

In order to predict the solid RP-1 thickness in the fuel manifold (Fig. 2), a simple one-dimensional thermal model¹² of the annulus wall separating LOX and RP-1 passages was built (Fig. 10). Results indicated that a solid film, averaging 0.009 inch, could develop. Flow area is reduced up to 20 percent as a result. Another design chart estimated a solid RP-1 layer 0.006 to 0.008 inch thick for the present operating conditions. Concerns about RP-1 freezing have led MSFC to instrument additional thermocouples to monitor RP-1 bulk temperature. Test data showed, as expected, that bulk RP-1 temperature inside a fuel annulus remained above 80 deg. F, exceeding the -50 deg. F freezing mark (Fig. 11).

For the pre-test calculations shown below, the hot-gas environment¹³ was numerically simulated by a separate in-house study. The resulting set of convective heat transfer coefficients were input as boundary condition for the SINDA model.

The injector faceplate (Fig. 2) is cooled during engine run by employing the two RP-1 jets to shield against the single LOX jet. A maximum surface temperature of about 200 deg. F was calculated. No data is available for model correlation but the post-test inspections revealed no damage. Extra margin was provided by the insulation effect of soot layer de-

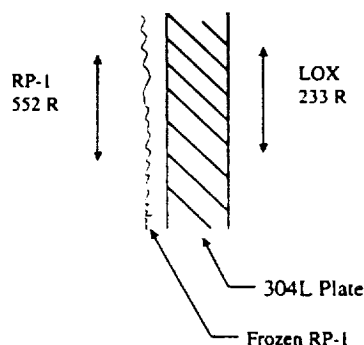


Fig. 10 1-D Model

positing during test.

The two-dimensional model (Fig. 9) was exercised to give temperature distribution on the combustion chamber wall. This is an area of concern because it is uncooled and a proper design for a heat shield bracket mounted on the external surface has to account for this hot boundary.

Figure 12 shows a sketch of the test article with external thermocouples. Shown by Figure 13 and Figure 14 are the test data and predictions. At its worst, the correlated model's results were within 50 degrees of test data. The maximum temperature, approximately 1100 F, was about the same for chamber locations that are 2.5 inches apart. This is probably due to the turbulent mixing process of the combustion products with the propellants having been completed, giving rise to flow uniformity the rest of the way.

Figure 15 shows the analysis results compared to the data at two locations near the faceplate. The maximum temperatures are different because unlike the situation in the preceding paragraph, mixing was incomplete.

Conclusions

The baseline design of the Fastrac gas generator was analyzed and the results were compared against applicable hot-fire data.

The maximum temperature on the chamber external surface was about 1100 deg. F. There were reasonable agreements between data and correlated numerical model.

Annulus flow area could be reduced by up to 20 percent although the RP-1 bulk temperature remained well above freezing during testing period.

The faceplate triplet design was adequately cooled, having suffered no erosion in any test thus far.

Acknowledgements

This work was supported by the NASA Office of Aeronautics and Space Transportation Technology (OASTT), Washington, D.C.

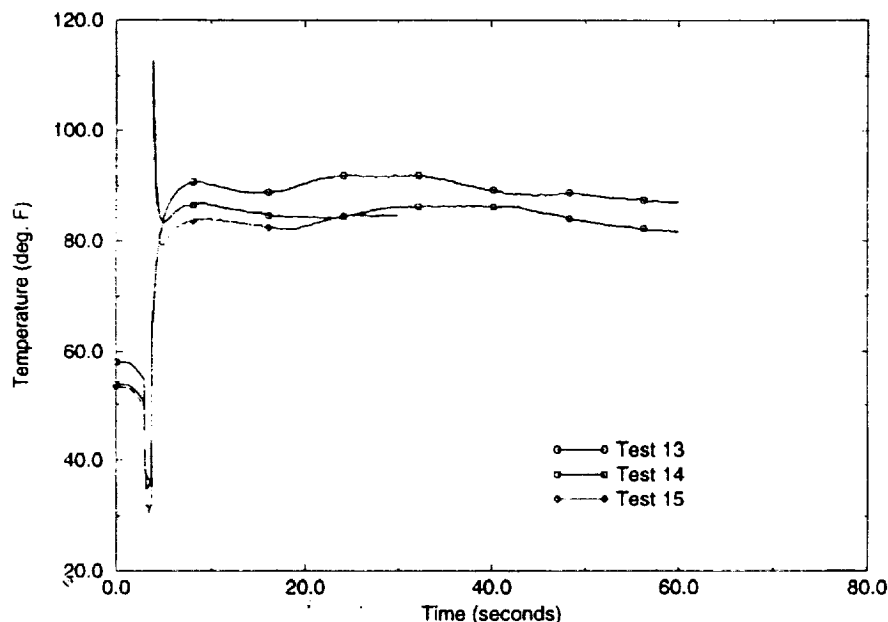


Fig. 11 RP-1 Manifold Temperature

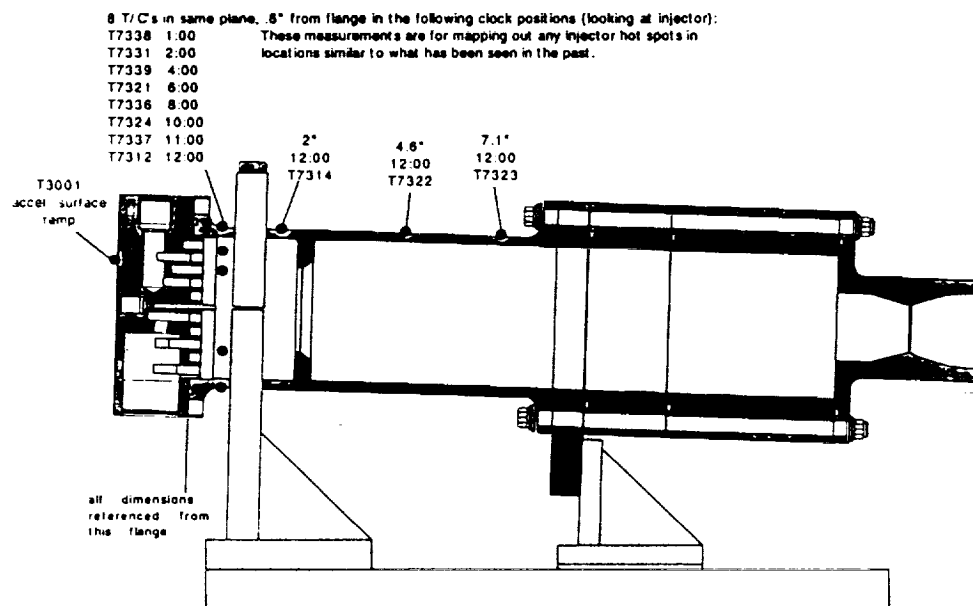


Fig. 12 Test article on test stand (Black dots denote thermocouple locations)

References

- ¹Anon., "NASA Studies Access to Space," Advanced Technology Team Volumes 1-4, 1993.
- ²Anon., "Low-Cost Boost Technology Project," *World Wide Web page address* <http://www.ies.msfc.nasa.gov/lcbl>.
- ³Garcia, R., "Computational Fluid Dynamics Analysis in Support of the Simplex Turbopump Design," *NASA CP-3292*, May 1994.
- ⁴Garcia, R., "Fluid Analysis of Pump Manifolds Designed for Cost," *JANNAF Propulsion Meeting*, 1996.
- ⁵Sparks, D., "Ablative Combustion Chamber Liner Feasibility Study," *NASA TM-108470*, 1994.
- ⁶Sgarlata, P. and Winters, B., "X-34 Propulsion System Design," *AIAA Paper 97-3304*, 1997.
- ⁷Anon., "Low-Cost Boost Technology Design Binder," Tech. Rep. Vol. 1, Book 3, NASA, 1997.
- ⁸Eckert, E., "Analysis of Heat and Mass Transfer," 1987.
- ⁹Anon., "P3/PATRAN User Manual," Tech. Rep. Vol. 1, 1993.
- ¹⁰Behee, R., "SINDA/G Tutorial Guide," Tech. rep., 1996.
- ¹¹Sanders, T., "Private Communication," 1997.
- ¹²Luong, V., "Private Communication," 1997.
- ¹³Canabal, F., "Private Communication," 1997.

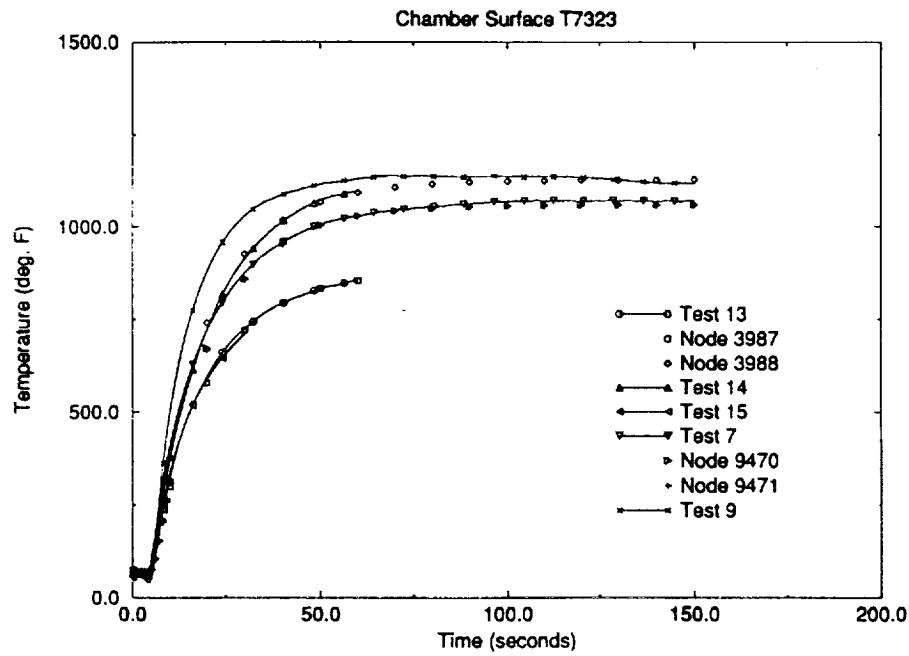


Fig. 13 Comparison vs. T7323 thermocouple data

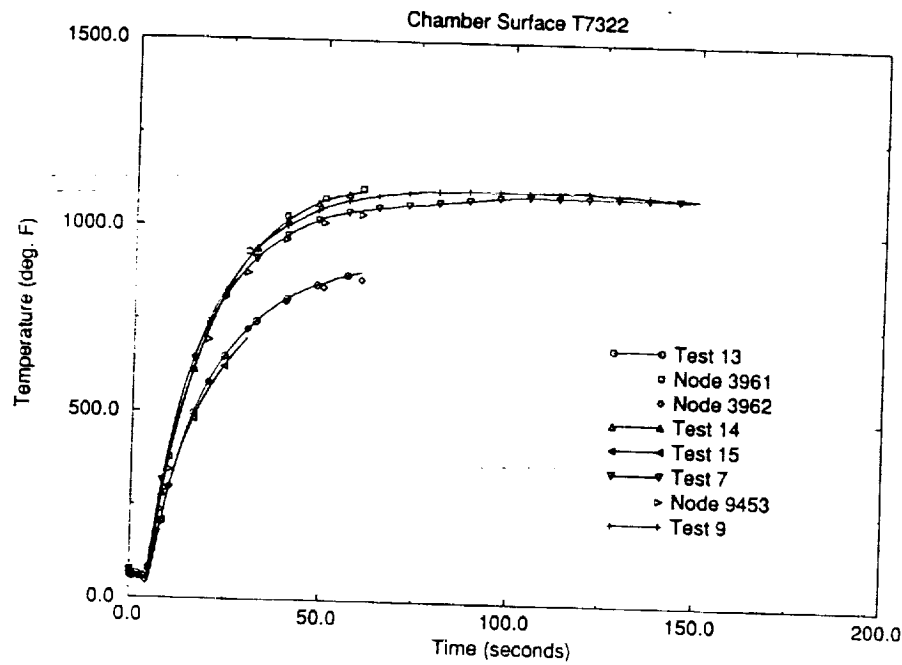


Fig. 14 Comparison vs. T7322 thermocouple data

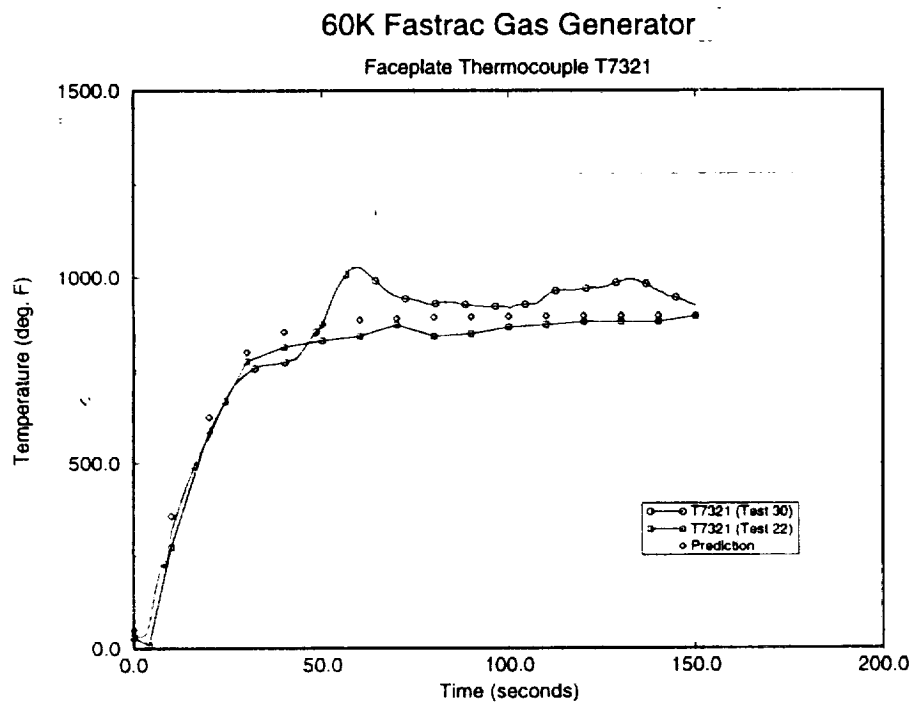
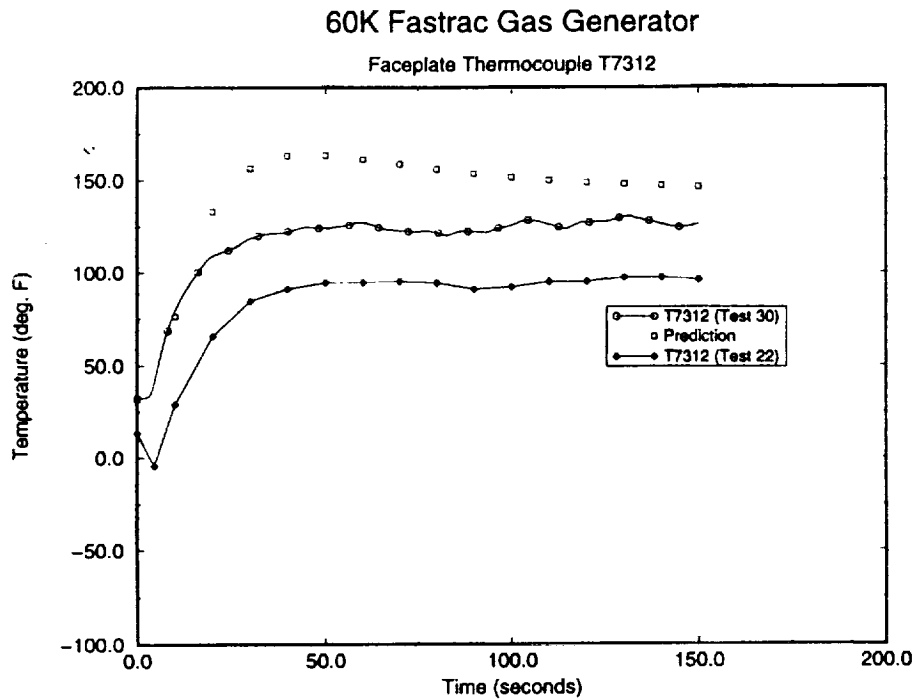


Fig. 15 Comparison vs. T7312 and T7321 thermocouple data